

# Exploring the optical and dielectrical properties of $\text{Zn}_{1-x}\text{Fe}_x\text{O}$ nano-crystal synthesized by SPM approach

Soufiane Benhamida<sup>1</sup>, Fayçal Baira<sup>2</sup>, Hazem Bouraoui<sup>3,4</sup>, Kaouther Baira<sup>2</sup>, Sara Zidani<sup>5</sup>, Yamina Benkrima<sup>6</sup>

<sup>1</sup> Faculty of Mathematics and Material Sciences, Radiation and Plasma and Surface Physics Laboratory (LRPPS), University of Kasdi Merbah Ouargla, 30000, Ouargla, Algeria.

<sup>2</sup> Department of sciences and technology, Faculty of technology, University of Batna 2, Alleys 53, Constantine Avenue. Fésdis, Batna 05078, Algeria.

<sup>3</sup> Laboratoire de Cristallographie, Université Mentouri, Constantine, Algérie.

<sup>4</sup> Univ. Ouargla, Fac. des Mathématiques et Sciences de la Matière, route de Ghardaia, Ouargla 30000, Algeria.

<sup>5</sup> Department of food technology, Laboratory of food Sciences (LSA), Institute of Veterinary and agricultural Sciences, University of Batna1 Hadj Lakhdar, Alleys May 19 Biskra Avenue, Batna, 05000, Algeria

<sup>6</sup> Ecole Normale Supérieure de Ouargla, 30000, Algeria.

\* Corresponding author. Email: benhamidas9@gmail.com

Submitted: 11/01/2024 ; Accepted: 05/04/2024

## Abstract

This study involved the preparation of  $\text{Zn}_{1-x}\text{Fe}_x\text{O}$  ( $x = 0, 0.02$ ) nano-crystal thin films utilising a straightforward spray pyrolysis method (SPM), with doping concentrations varied from 0 to 2 wt.% at a constant substrate temperature of 350 °C. The influence of Fe-doping concentration on the optical and dielectrical properties of ZnO thin films was examined and addressed. The optical properties revealed that the films with Fe-doping concentration (2 wt.%) showed high transmittance and wide band gap than the undoped ZnO samples. The estimated band gap showed a decreased from 3.27 eV to 3.09 eV as Fe doping concentration increases. The refractive index of the films exhibited a significant variation with increasing of doping. The interaction between free electrons and incident photons is indicated by the change in the real and imaginary parts of dielectric constants with photon energy.

**Key words:** Thin films, Zinc oxide, spray pyrolysis; Optical properties, dielectrical properties

## 1. Introduction

For the past 15 years, the most exciting area of materials research has been transparent conducting oxide (TCO) thin film technology. A vast number of researchers exist. Utilizing differentiated TCO materials and various methodologies for their deposition in appropriate applications has been implemented [1]. TCOs provide both great transparency and low electrical resistance. The electrical band structure of solids determines their optoelectronic capabilities. Tin oxide ( $\text{SnO}_2$ ), Indium oxide ( $\text{In}_2\text{O}_3$ ), Zinc oxide ( $\text{ZnO}$ ), Gallium oxide ( $\text{Ga}_2\text{O}_3$ ) etc are the different TCOs available.  $\text{ZnO}$  is a significant II-VI compound semiconductor characterized by a wide energy band gap of 3.37 eV and a substantial exciton binding energy of 60 meV at ambient temperature. The compound is mostly ionic, featuring ionic radii of 0.74 Å for  $\text{Zn}^{2+}$  and 1.40 Å for  $\text{O}^{2-}$ , with a space group of P63mc [2]. Under artificial conditions,  $\text{ZnO}$  typically crystallizes in a wurtzite form. It is extensively utilized for high transmittance, conductive oxide coatings in solar cells, gas sensors, UV photodetectors, and

bulk acoustic wave resonators [3-6]. ZnO is an effective piezoelectric material, exhibiting chemical stability and biocompatibility. Owing to its extensive band gap and elevated exciton binding energy [7], it is advantageous for UV/blue emission devices [8]. Doping is a significant procedure that aids in enhancing and controlling the structural, electrical, and optical properties of ZnO thin films. Among metal dopants, iron (Fe) is chemically stable and exists in two oxidation states,  $\text{Fe}^{2+}$  and  $\text{Fe}^{3+}$ , with ionic radii of 0.78 Å and 0.64 Å, respectively, which are comparable to the ionic radius of  $\text{Zn}^{2+}$  (0.74 Å) [9]. Consequently, it can readily occupy Zn lattice positions, either substitutionally or interstitially, without disrupting the crystal structure of ZnO, thereby enhancing its conductivity through an increased number of charge carriers. Diverse physical and chemical methodologies such as sol-gel, spray pyrolysis, DC magnetron sputtering, hydrothermal process, and electrodeposition despite the various methods employed to fabricate ZnO films [10-14]. Consequently, this study employs a straightforward, vacuum-free, and economical spray pyrolysis method (SPM) to deposit Fe-doped ZnO thin films, and the optical and dielectrical properties of the resultant layers were examined comprehensively.

## 2. Experimental details and characterization

We employed spray pyrolysis method (SPM) for the preparation of undoped and Fe-doped ZnO films. In this method, zinc acetate dehydrate ( $\text{Zn}(\text{COOCH}_3)_2 \cdot 2\text{H}_2\text{O}$ ), hydrated ferric chloride  $\text{FeCl}_3 \cdot 6\text{H}_2\text{O}$ , double-distilled water were used as precursor for zinc, iron and solvent respectively. Briefly, zinc acetate dehydrate was dissolved in a 30 ml of double-distilled solution at a room temperature where the concentration of zinc acetate was 0.1 M. Here, samples  $\text{Zn}_{1-x}\text{Fe}_x\text{O}$  ( $x = 0, 0.02$ ) with different Fe contents were prepared. Then, the solution was stirred at 50°C with a magnetic stirrer for 20 minutes to yield a clear homogeneous solution. The substrates consisted of small glass slides measuring 75×25×1.1 mm<sup>3</sup> (R217102). The normal cleaning technique for glass substrates before the deposition process involved rinsing them in distilled water and acetone for ten minutes and then drying them with compressed air. The as-prepared solution was sprayed onto heated substrates fixed at 350°C, the distance between spray nozzle and substrate (15 cm), carrier gas flow (1 kg/cm<sup>2</sup>), solution flow rate (2 ml/min). Finally, the fabricated films were allowed to cool gradually at room temperature. To investigate the optical and dielectrical properties of all prepared samples, the Cray 100 UV-vis-NIR spectrophotometer Agilent Technologies in the spectral range of 300–800 nm were used.

## 3. Result and discussions

### 3.1 Optical transmission and optical energy band gap

The UV-Vis-NIR transmission spectra of  $\text{Zn}_{1-x}\text{Fe}_x\text{O}$  ( $x = 0, 0.02$ ) films with different Fe contents are presented in Fig. 1. One can be seen, from undoped ZnO films that the sample shows optical transmittance of about > 93% whereas from Fe-doped (2 wt.%) exhibited high optical transmittance (>98%) than the undoped ZnO films in the visible region. This variation can be assigned to the changes in both the crystalline quality and roughness of film surface [15]. The optical transmission decreases quickly in the wavelength range 350–400 nm in the UV region owing to sharp absorption. This behavior corresponding to the onset fundamental absorption edge of ZnO due to the transition between the valence band and the conduction band.

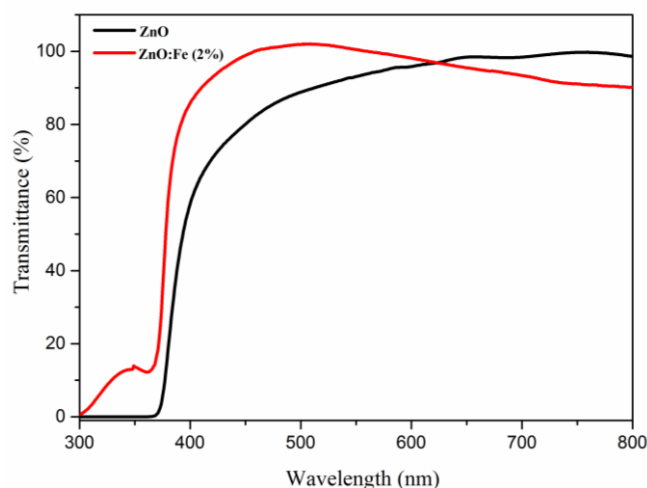


**Fig. 1: transmittance spectra of undoped and 2 wt.% Fe-doped ZnO films.**

The optical band gap of  $\text{Zn}_{1-x}\text{Fe}_x\text{O}$  ( $x = 0, 0.02$ ) samples was deduced by employing the Tauc relation corresponding to the direct band gap materials. The absorption coefficient is given by [16]:

$$\alpha = \frac{2.303 \cdot A}{t} \quad (1)$$

where  $A$  is absorbance and  $t$  is thickness of the film.

The Optical energy gap  $E_g$  and absorption coefficient  $\alpha$  are related from the Tauc's relation [16]:

$$(\alpha h\nu) = K (h\nu - E_g)^{\frac{1}{n}} \quad (2)$$

where  $\alpha$  is the absorption coefficient,  $(h\nu)$  is the photon energy, and  $K$  is a constant and  $n$  is the constant that is equal to 2, 1/2, 2/3 and 1/3 for allowed direct, allowed indirect, forbidden direct and forbidden indirect transitions respectively. The direct optical band gaps were obtained by the least square fitting from the linear portion of  $(\alpha h\nu)^2$  versus  $(h\nu)$  plot, as is presented in Fig. 2. The evaluated band gaps are 3.27 eV and 3.09 eV for undoped, Fe= 2 wt doped ZnO films respectively. The band gap of the ZnO decreased by Fe doping. This decrease in the  $E_g$  value is an indicator of the modification in the ZnO structure after doping with Fe ions and is linked with the creation of localized states in the band gap [17-19].

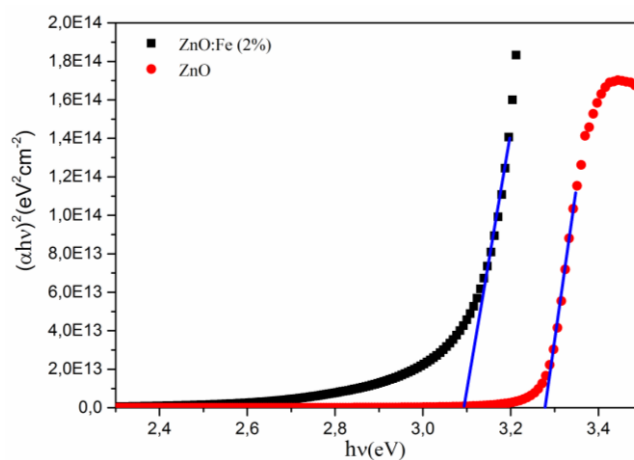


**Fig.2: Estimation of band gap energy ( $E_g$ ) from Tauc's relation of undoped and 2 wt.% Fe-doped ZnO films.**

### 3.2 Refraction index and extinction coefficient

One significant dimensionless optical constant of a substance that describes how electromagnetic waves travel through it is its refractive index ( $n$ ). The propagation of light through the medium is contingent upon its wavelength  $\lambda$ . As light propagates in a lossy medium, it experiences attenuation and dispersion, resulting in energy loss due to scattering, photo-generation, and lattice wave creation, among other phenomena. the index of refraction ( $n$ ) and extinction coefficient ( $k$ ) were determined by the following equations [20]:

$$k = \frac{\alpha\lambda}{4\pi} \quad (3)$$

and

$$n = \left( \frac{1-R}{1+R} \right) + \sqrt{\frac{4R}{(1-R)^2} - k^2} \quad (4)$$

where  $R$  is the reflectance of the medium. Figure 3 illustrate the variation of the refractive index as function the wavelength ranged from 300 nm to 800 nm of undoped and Fe doped ZnO films . It can be observe that refractive index decreases with increase of wavelength in a similar manner for each film. One can also note that as doping with Fe ions increases refractive index decreases compared with undoped ZnO samples. The decay in the refractive index values towards longer wavelength may be ascribed to the impact of ZnO lattice absorption.

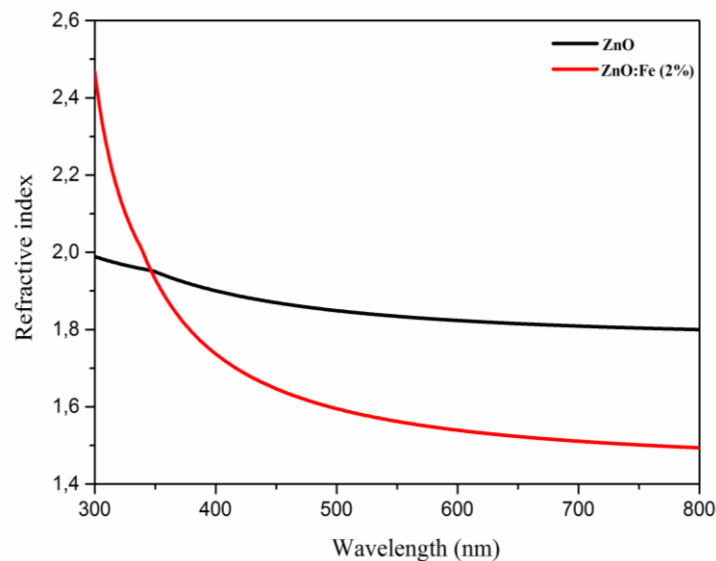


**Fig. 3: Refractive index as function of wavelength of undoped and 2 wt.% Fe-doped ZnO films.**

The extinction coefficient indicates the energy lost owing to scattering or absorption by molecules and particles within the substance. Fig. 4 represents extinction coefficient as function of wavelength of undoped and 2 wt.% Fe-doped ZnO. It is evident that the extinction coefficient decreases with increases of the incident photon energy in all prepared samples. Also the lower values extinction coefficient indicates that the portion of light lost is attributable to the scattering that causes a decrease in absorbance [21].

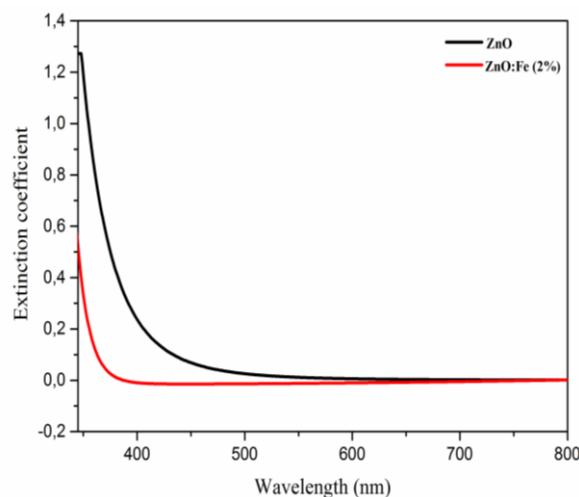


**Fig. 4:** Extinction coefficient as function of wavelength of undoped and 2 wt.% Fe-doped ZnO films.

### 3.3 Dielectric constants

The real ( $\epsilon_1$ ) and imaginary ( $\epsilon_2$ ) components of dielectric constants are crucial factors as they convey insights on optical behavior and the dispersion factor. The real  $\epsilon_1$  and imaginary  $\epsilon_2$  components of the dielectric constants can be obtained using the following equations [22].

$$\epsilon_1 = n^2 - k^2 \quad (5)$$

and

$$\epsilon_2 = 2nk \quad (6)$$

Fig. 5 shows the dependences of The real ( $\epsilon_1$ ) and imaginary ( $\epsilon_2$ ) components of dielectric constants as function of photon energy of  $\text{Zn}_{1-x}\text{Fe}_x\text{O}$  ( $x = 0, 0.02$ ) films. The obtained values of  $\epsilon_1$  and  $\epsilon_2$  are found to increase as photon energy increases. The fluctuation of the real and imaginary components of dielectric constants with photon energy signifies the interaction between free electrons and incident photons. The value of  $\epsilon_1$  is significantly higher than  $\epsilon_2$ ; this comparison finding suggests the dependency of  $\epsilon_1$  on  $n$ , where  $n > k$ , as illustrated in Fig. 3 and Fig. 4. The real component of the dielectric constant increases sharply with rising  $h\nu$ , whereas the imaginary component remains relatively escalates rapidly as photon energy rises.

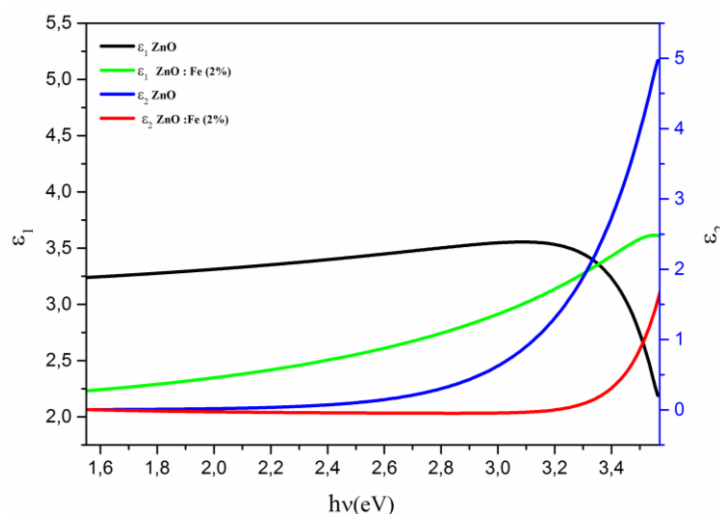


**Fig. 5:** The real  $\epsilon_1$  and imaginary  $\epsilon_2$  parts of the complex dielectric constant as function of photon energy of undoped and 2 wt.% Fe-doped ZnO films.

#### 4. Conclusion

The spray pyrolysis deposition method has been employed to fabricate  $\text{Zn}_{1-x}\text{Fe}_x\text{O}$  ( $x = 0, 0.02$ ) nano-crystal thin films on glass substrates at  $350^\circ\text{C}$ . The optical, and dielectric properties of grown thin films have been examined to understanding the effect of Fe doping of ZnO thin films. The optical transmittance demonstrate that the undoped ZnO films shows optical transmittance of about  $> 93\%$  whereas from Fe-doped (2 wt.%) exhibited high optical transmittance ( $>98\%$ ) in the visible region. Optical analysis indicated direct allowed transitions with  $E_g$  values decreases from 3.27 eV to 3.09 eV as the increase of Fe ions, indicating the semiconducting nature. Furthermore, the refractive index of the films was found to vary strongly with increases of Fe ions. The variation of the real and imaginary parts of dielectric constants with photon energy indicates the interaction between the free electrons and the incident photons. The synthesized films, with optimized optical band gaps, elevated refractive indices, and minimal Fe ion doping concentration, are suitable for anti-reflection coatings and optoelectronic applications.

#### References

- [1] M. T. Greiner and Z. H. Lu, "Thin-film metal oxides in organic semiconductor devices: Their electronic structures, work functions and interfaces," *NPG Asia Materials*, vol. 5, pp. 55-16, 2013.
- [2] Chakrabarti S.; Ganguli D.; and Chaudhuri S.; Photoluminescence of ZnO nanocrystallites confined in sol–gel silica matrix. *J. Phys. D: Appl. Phys.* 2003, 36, 146-151.
- [3] G. Regmi, S. Velumani, Radio frequency (RF) sputtered  $\text{ZrO}_2\text{-ZnO-TiO}_2$  coating: An example of multifunctional benefits for thin film solar cells on the flexible substrate, *Solar Energy* 249, (2023), 301-311.
- [4] V.S. Chandak, M.B. Kumbhar, P.M. Kulal, Highly sensitive and selective acetone gas sensor-based La-doped ZnO nanostructured thin film, *Materials Letters* 357(2024)135747.
- [5] Samer H. Zyoud, Ahmad Fairuz Omar, Investigating the role of Ag-doped ZnO thin films in UV photodetectors produced via laser assisted chemical bath growth technique, *Physica B: Condensed Matter* 694 (2024), 416406.
- [6] Jitendra Singh, Saurabh Kumar Gupta, Vinita, Room temperature operating formaldehyde sensor based on n-type ZnO functionalized surface acoustic wave resonator, *Sensors and Actuators A: Physical* 365 (2024), 114818.
- [7] Mishra A. K.; Chaudhuri S. K.; Mukherjee S.; Priyam A.; Saha A.; and Das D.; Characterization of defects in ZnO nanocrystals: Photoluminescence and positron annihilation spectroscopic studies. *J. Appl. Phys.*, 2007, 102, 103514-6.
- [8] Maensiri S.; Laokul P.; and Promarak V.; Synthesis and Optical Properties of Nanocrystalline ZnO Powders by a Simple Method Using Zinc Acetate Dihydrate and Poly (Vinyl Pyrrolidone). *J. Crys. Growth*. 2006, 289, 102-106.
- [9] T. Srinivasulu, K. Saritha, K.T. Ramakrishna Reddy, Synthesis and Characterization of Fe-doped ZnO Thin Films Deposited by Chemical Spray Pyrolysis, *Modern Electronic Materials* 3, 2(2017) 76-85.
- [10] Faran Baig, Ghulam Sarwar Butt, Impact of copper doping on optical, UV induced wettability and photo-catalytic properties of sol-gel synthesized ZnO thin films, *Optik* 288(2023) 171196.
- [11] Aeshah Alasmari, Abanob A. Awad, Ahmed A. Aboud, Investigating the influence of yttrium doping on physical properties of ZnO thin films deposited via spray pyrolysis, *Optical Materials* Volume 148, February 2024, 114899.
- [12] Cristian L. Terán, Jorge A. Calderón, Heiddy P. Quiroz, A. Dussan, Optical properties and bipolar resistive switching of ZnO thin films deposited via DC magnetron sputtering, *Chinese Journal of Physics*, 74 (2021) 1-8.
- [13] Hussein M. Hussein, Photosensitive analysis of spin coated Cu doped ZnO thin film



synthesized by hydrothermal method, *Results in Optics*, 13 (2023)100543.

[14] Abdul Hadi Ismail, Abdul Halim Abdullah, Yusran Sulaiman, Physical and electrochemical properties of ZnO films fabricated from highly cathodic electrodeposition potentials, *Superlattices and Microstructures*, 103 (2017)171-179.

[15] S.M. Salaken, E. Farzana, J. Podder, Effect of Fe doping on the structural and optical properties of ZnO thin films prepared by spray pyrolysis, *J. Semicond.*, 34 (2013), 1-6.

[16] T. Srinivasulu, K. Saritha, K.T. Ramakrishna Reddy, Synthesis and characterization of Fe-doped ZnO thin films deposited by chemical spray pyrolysis, *Modern Electronic Materials* 3, 2(2017)76-85.

[17] A.A. Ebnalwaled, A. Thabet, Controlling the optical constants of PVC nanocomposite films for optoelectronic applications, *Synth. Met.* 220 (2016) 374–383.

[18] S.B. Aziz, H.M. Ahmed, A.M. Hussein, A.B. Fathulla, R.M. Wsw, R.T. Hussein, Tuning the absorption of ultraviolet spectra and optical parameters of aluminum doped PVA based solid polymer composites, *J. Mater. Sci. Mater. Electron.* 26 (2015) 8022–8028.

[19] S.B. Aziz, S. Hussein, A.M. Hussein, S.R. Saeed, Optical characteristics of polystyrene based solid polymer composites: effect of metallic copper powder, *Int. J. Met.* 2013 (2013).

[20] K. S. Usha, R. Sivakumar, and C. Sanjeeviraja. Optical constants and dispersion energy parameters of NiO thin films prepared by radio frequency magnetron sputtering technique. *Journal of Applied Physics* 114: 123501 (2013).

[21] H. E. Atyia, S. S. Fouad, Pankaj Sharma, A. S. Farid, N. A. Hegab, Optical, dielectric and opto-electrical study of Se-Te-Ge glassy thin films, *Journal Of Optoelectronics And Advanced Materials*, 20, 5 (2018) 319 – 325.

[22] Mohammed, M.I., S.S. Fouad, and N. Mehta, Dielectric relaxation and thermally activated ac conduction in (PVDF)/(rGO) nano-composites: role of rGO over different fillers. *Journal of materials Science: Materials in Electronics*, 2018. 29(21): 18271- 18281.